Available online at www.sciencedirect.com
SCIENCE DIRECT
Polymer 46 (2005) 10139–10147
polymer
www.elsevier.com/locate/polymer

Thermal decomposition of alkyl ammonium ions and its effects on surface polarity of organically treated nanoclay

Dhawal Dharaiya, Sadhan C. Jana*

Department of Polymer Engineering, The University of Akron, Akron, OH 44325-0301, USA

Received 13 July 2005; received in revised form 29 July 2005; accepted 3 August 2005
Available online 25 August 2005

Abstract

The surface free energy and surface polarity of organically modified montmorillonite clay change when exposed to elevated temperatures. This was verified in this study using contact angle measurements and Wu's harmonic-mean equation. It was observed that the surface polarity of organically modified clay measured from the values of contact angle of water and diiodomethane reduced significantly owing to thermal degradation of the organic modifier of clay, the latter was confirmed by Fourier transform infra-red spectroscopy. As a consequence, nonpolar polymer, polypropylene (PP), was found to spread more on heat treated surface of organically modified clay than a polar polymer, polyamide 6 (PA6). The ramification of these phenomena on blending of PP, PA6, and organically modified clay is discussed.

Keywords: Nanoclay; Thermal decomposition; Contact angle

1. Introduction

Inorganic filler particles such as talc, mica, fumed silica, and layered silicates are widely used as reinforcement of polymers; of these, nanosized varieties are gaining popularity due to their potential in offering superior properties at much smaller loadings [1–3]. For example, polyamide 6 (PA6) reinforced with 5 wt% organically modified nanoscale layered silicate clays provide 168% increase in tensile modulus, 87 °C increase in heat distortion temperature, and 40% decrease in water permeability over PA6 [1,2]. Nanoscale layered silicate clays are organically modified by exchange of intra-gallery cations with alkyl ammonium ions, which in turn facilitate diffusion of monomers or polymer chains during preparation of nanocomposites [1–4].

Several nanocomposite preparation methods have been considered in literature [3,5 and references therein]. Among these, melt intercalation method has been found very convenient [6,7]. In melt intercalation, clay particles are directly combined with the polymer in conventional mixing equipments. A drawback of melt intercalation method, however, is elevated polymer mixing temperatures, which can potentially cause thermal decomposition of commonly used alkyl ammonium ions in modified clays [8–11]. Xei et al. [8] used thermogravimetric analysis coupled with mass spectrometry to monitor thermal decomposition products from clays treated with a series of alkyl ammonium ions. These authors successfully detected small molecular species as decomposition products, such as carbon dioxide, short chain alkanes, alkenes, etc. It was observed that thermal decomposition of alkyl ammonium ions starts at temperatures as low as 180 °C; a majority of decomposition, however, occurs between 200 and 500 °C. Note that many thermoplastic polymers are processed at temperatures in the range of 200–250 °C and some thermosetting materials are cured at temperatures above 200 °C. Consequently, clay–polymer mixing or curing in these cases can subject alkyl ammonium ions to thermal decomposition, which in turn can exert potential detrimental effects on product properties and performance. Some detrimental effects of thermal decomposition have already been identified in literature, e.g. in the form of discoloration of polycarbonate–clay [12] and polyamide–clay composites [13] and in plasticization and reduction of glass transition temperature of crosslinked epoxy–clay systems [14]. Additionally, VanderHart et al. [10] concluded that combination of shear stress involved in

* Corresponding author. Fax: +1 330 258 2339.
E-mail address: janas@uakron.edu (S.C. Jana).

0032-3861/$ - see front matter © 2005 Published by Elsevier Ltd.
doi:10.1016/j.polymer.2005.08.027

mixing and mixing temperature causes decomposition of alkyl ammonium ions in PA6-clay nanocomposites. However, these authors observed no significant effect of decomposition on clay dispersion.

Another effect of thermal decomposition of alkyl ammonium ions can be realized in the form of alteration of clay surface energy, which may exert detrimental effects on clay particle dispersion and on final morphology of polymer blends, especially if polar and non-polar polymers are blended in the presence of organically modified clay. To the best of our knowledge, this issue has not been explored in detail in literature. It has been recently observed that organically modified layered silicate particles helps reduce the domain size of dispersed polymer in immiscible polymer blends [15–22], purportedly via compatibilization effects [15,16]. In this context, a change in polarity of organically modified clay particles due to thermal decomposition may produce counterintuitive results.

This paper deals with determination of surface free energy and polarity of organically modified montmorillonite clay from contact angle measurements and Wu's harmonic mean equation [23,24] before and after thermal decomposition of alkyl ammonium ions using one commercial organically modified clay. The clay surface was prepared by exposing clay discs to elevated temperatures for the duration of time as is encountered in typical polymer–clay mixing experiments.

Owens and Wendt [25] estimated surface free energy of solids by measuring contact angle of liquids of known surface tensions. They showed that the surface energy of the solid can be resolved into dispersion and hydrogen bonding-dipole components. Wu and Brzozowski [23] used contact angle data of water and diiodomethane on pressed organic pigments to calculate surface free energy and polarity using harmonic mean equation [24] and found reasonable agreement between measured values of surface free energy and those estimated from the parachor [26,27]. Le Pluart et al. [28] calculated dispersive and polar components of surface free energy of clay surfaces as function of modification by alkyl ammonium ions of different chain lengths. These authors showed using contact angle data and thermogravimetric analysis that longer chain alkyl ammonium ions cover the clay surfaces and that excess ions are physisorbed outside the clay galleries although Xie et al. [8] proposed that excess ions remain inside the clay galleries.

2. Experimental

2.1. Materials

The organically modified nanoclay used in the study is Closite®30B, obtained from Southern Clay Products (Gonzales, TX). Cloisite® 30B is a natural montmorillonite clay modified with $N^+(CH_2CH_2OH)_2(CH_3)T$ quaternary ammonium ion derived from tallow amine, where T represents an alkyl group with approximately 65% $C_{18}H_{37}$, 30% $C_{16}H_{33}$, and 5% $C_{14}H_{29}$ [29]. Approximately, 90 milliequiv of quaternary ammonium ions are present per 100 g of Cloisite® 30B particles. Unmodified natural montmorillonite, Cloisite®NA+, was also obtained from Southern Clay Products. Fig. 1 presents scanning electron micrograph of clay particles showing agglomerates of 5–20 μm size. The clay particles were dried in vacuum oven at 80 °C for 24 h. As individual clay particles were of very small size, we used compressed clay disks for contact angle measurements. Approximately 3.5 g dried clay powder was placed inside a cylindrical metal chamber with inner diameter 25.4 mm and compacted by a plunger. The plunger was moved with a constant crosshead speed of 10 mm/min until the maximum compaction force of 15 kN was reached. A pair of Teflon washer was used to ensure easy removal of the disks and to produce smooth surfaces. The disks appeared smooth when inspected by optical microscopy, although scanning electron microscopy (SEM) revealed largest asperities of the order of less than 5 μm

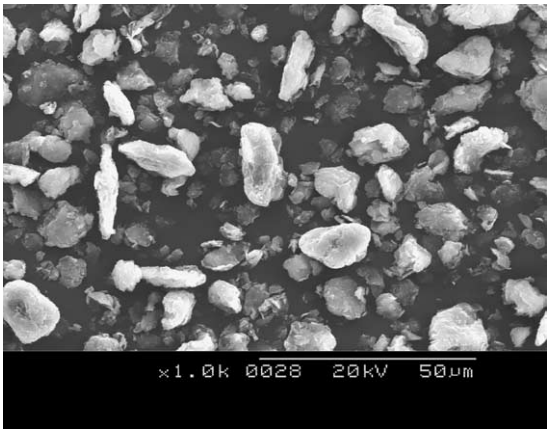

Fig. 1. SEM image of as received Cloisite® 30B particles.

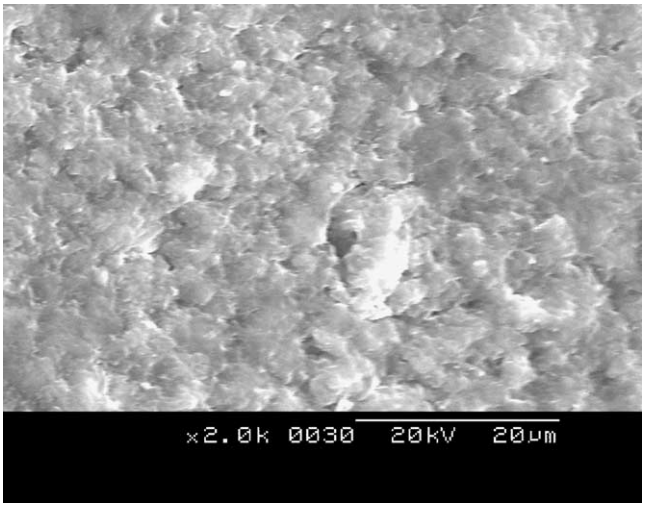

Fig. 2. SEM image of surface of Cloisite® 30B pressed in to disk.

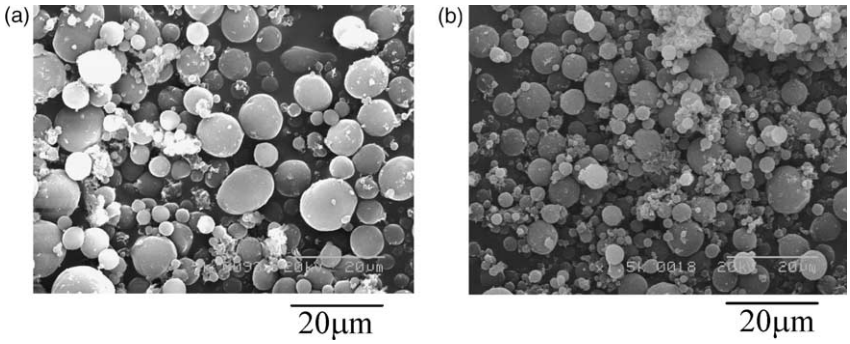

Fig. 3. SEM images of PP droplets obtained after mixing for a total strain (γ) of (a) 1334 and (b) 5320. Values of strains were computed based on a mean shear rate of 6.15 s^{-1} and mixing time.

(Fig. 2). These asperities, however, did not have any effect on reproducibility of contact angle data.

Two immiscible polymers, polyamide 6 (PA6) and polypropylene (PP) were used for contact angle measurements and to produce blends with nanoclay. Polyamide 6, grade Zytel® 7301 NC010 with specific gravity 1.13 and melting point (T_m) ~220 °C, was supplied by DuPont Engineering Polymers and polypropylene, grade PP 51S30V with specific gravity 0.91, melt flow index 30, and T_m ~165 °C was obtained from Equistar Chemicals. Polymers were dried in vacuum oven at 80 °C for 24 h before experiments.

In our prior work [30,31] on PP/PA6/clay blends, we studied the effects of nanoclay on morphology development of PP-phase. The Cloisite® 30B clay particles were initially mixed with PP in a weight ratio of 90:10 at 220 °C for 7 min and the PP–clay compound (PPCL) was mixed with PA6 in a weight ratio of 10:90 in a chaotic mixer at 250 °C for a maximum time-period of 10 min. It was observed that PP-phase produced lamellas, fibrils, and droplets as in systems without clay particles [32–34]. However, clay particles remained in PP-phase till the fibrils broke into droplets and subsequently migrated to PA6-phase. Fig. 3 presents scanning electron micrographs of droplets of PP-phase after extraction of PA6 with formic acid. These droplets were subjected to thermogravimetric analysis to determine the quantities of clay particles contained in them and to assess if migration of clay particles from PP droplets to PA6-phase had occurred. It is seen in Fig. 4 that PP droplets gradually lost clay particles due to migration to PA6 phase. These migrated clay particles were intercalated by PA6 chains as evident from X-ray diffraction patterns of PP–PA6–clay compound presented in Fig. 5. Note from the X-ray diffraction pattern presented in the inset of Fig. 5 that PPCL compound shows clay peak at slightly higher value of $2\theta = 6.3°$ compared to a peak of $2\theta = 5.2°$ for Cloisite® 30B clay. A detailed analysis of various stages of morphology development in PP–PA6–clay compound is presented elsewhere [30,31]. Clay discs used in the present study were prepared following the same thermal history as experienced by the clay particles during mixing with PP and PA6 as described above. Diiodomethane from Alpha Aesar and deionized water were used for contact angle measurements at room temperature with heat treated clay discs.

2.2. Contact angle measurements

As clay, PP, and PA6 were mixed at 250 °C in our prior work [30,31], we chose the same temperature to measure contact angle of PP and PA6 pellets on clay discs. Clay discs were kept in oven under nitrogen purge at 250 °C for 1 h to affect thermal decomposition of the quaternary ammonium ions. A small polymer pellet of ~2 mm diameter and ~3 mm length was kept on the surface of clay disk and the disk was kept at 250 °C for another 1 h in the oven under nitrogen purge. This time of 1 h was necessary to obtain complete melting of the polymer and to attain equilibrium shape by the polymer drop on the clay surface. Note that additional thermal decomposition of the quaternary ammonium ions occurred during these experiments. The clay discs with polymer drops were carefully taken out of the oven and quenched instantaneously by dipping in liquid nitrogen to preserve the shape of molten polymer droplet on

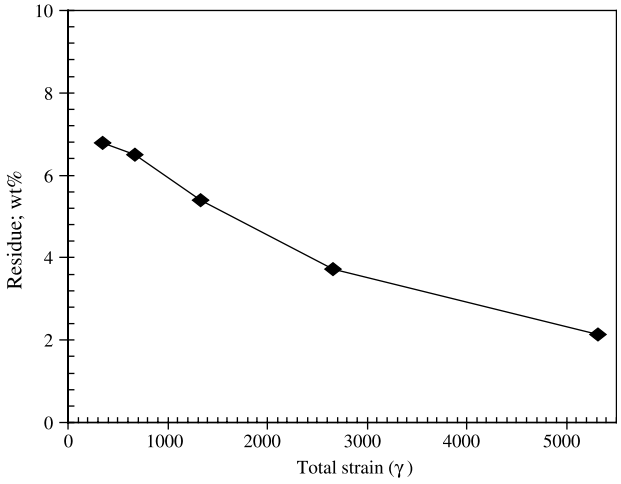

Fig. 4. TGA residue of PP-droplets expressed as weight percent of original droplet weight. Values of strains were computed based on a mean shear rate of 6.15 s^{-1} and mixing time.

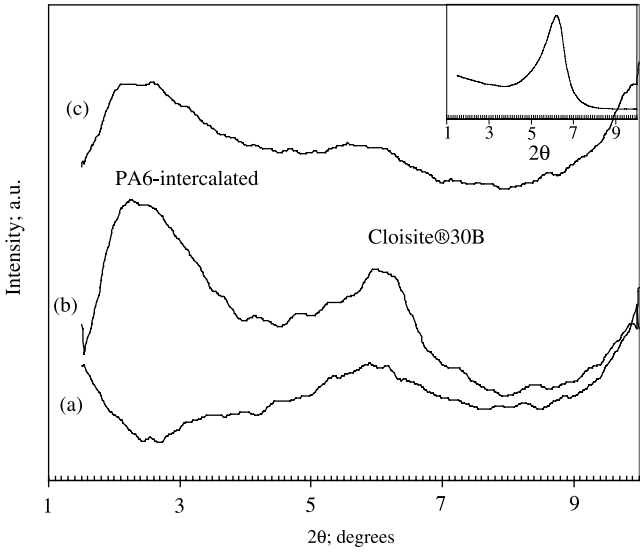

Fig. 5. X-ray diffraction scans of PA6–PPCL compound mixed for total strains of (a) 341, (b) 667, (c) 2662. Values of strains were computed based on a mean shear rate of 6.15 s^{-1} and mixing time. Clay peak and peak due to intercalated PA6 chains are shown. Inset presents X-ray diffraction scan of PPCL compound.

clay surface. Some blank clay disks were subjected to the same heat treatment, dried in vacuum oven, and stored for contact angle measurements using water and diiodomethane.

Clay disks were also heated in oven under nitrogen purge for different times to emulate thermal decomposition of clay particles in mixing experiments as reported in our earlier work [30,31]. The contact angles of sessile drops of water and diiodomethane on such heat treated clay discs were measured using a FTA200 device from First Ten Angstroms (Portsmouth, VA). A 5 ml syringe filled with water or diiodomethane was attached to a motor driven plunger. The liquid was dispensed from the syringe at a rate of 1 μl/min till a drop was produced at the tip of the needle attached to the syringe. The clay disk was raised and the drop was transferred to the surface of the clay disk without splashing and deformation of the drop. For each heat treated disk, 8–10 measurements were taken to obtain reproducible results. The value of contact angle was determined from digitized optical images of the liquid drop. For each image, the contact angle values were calculated on both edges using software supplied with the instrument. In addition, contact angle values were calculated by considering the drop as a part of the sphere. It was found that both methods produced results with reasonable agreement. The values of total surface energy (γ), and the polar (γ^{p}) and dispersion (γ^{d}) components of total surface energy was computed from contact angle values using Wu's harmonic-mean equation [23,24] as in Eq. (1).

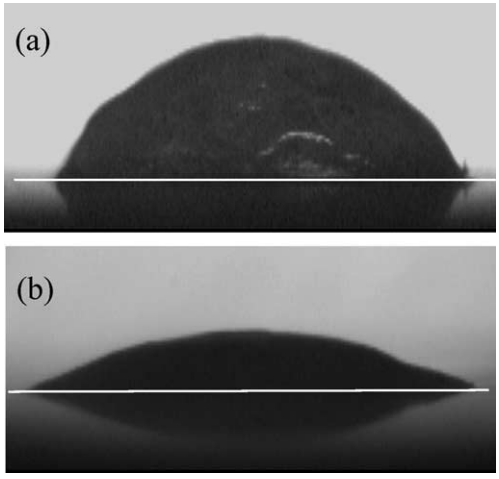

Fig. 6. Optical image of drop of (a) PA6 and (b) PP on clay surface obtained at 250 °C. The measured value of contact angle for PA6 was 73.5° and for PP was 30°.

$$\gamma_{12} = \gamma_1 + \gamma_2 - \frac{4\gamma_1^{d}\gamma_2^{d}}{\gamma_1^{d} + \gamma_2^{d}} - \frac{4\gamma_1^{p}\gamma_2^{p}}{\gamma_1^{p} + \gamma_2^{p}} \quad (1)$$

In Eq. (1), γ_{12} is the interfacial energy, γ_i is the surface free energy of ith component, γ_i^{d} is dispersion (non-polar) component of the surface free energy, and γ_i^{p} is the polar component of the surface free energy. A more detailed procedure for using contact angle data of two liquid and Wu's harmonic mean equation to compute surface free energy values is described elsewhere [24]. The following numerical values of the surface energy of components were used for pure liquids: $\gamma^{d}=21.8$ dyn/cm and $\gamma^{p}=50.7$ dyn/cm for water and $\gamma^{d}=44.1$ dyn/cm and $\gamma^{p}=6.7$ dyn/cm for diiodomethane [24]. The value of surface polarity (p) of a clay specimen was computed as the ratio of polar (γ^{p}) component of free energy to surface free energy (γ). The surface free energy of various polymer components was also determined in similar manner using water and diiodomethane on solid polymeric surfaces. For this purpose PA6, PP, and PPCL were molded into smooth sheets by compression molding. The surfaces were cleaned with alcohol and dried in vacuum oven before experiment.

2.3. X-ray diffraction (XRD)

XRD scans of heat treated clay and PP/PA6/clay compound were performed using Rigaku X-ray diffractometer at an acceleration voltage of 50 kV and current of 150 mA. The samples were scanned in reflection mode in 2θ range of 1.5–10° in steps of 0.02°. These measurements were used to reveal if decomposition of quaternary ammonium ions had any effect on clay height between clay galleries and if polymer chains intercalated the clay galleries.

2.4. FTIR analysis

FTIR spectra of clay discs heated for various times were taken using a Bio-Rad FTS-125 spectrometer equipped with

a Harrick diamond cell accessory. This was done to evaluate the effect of heat treatment on clay particles. The samples were scanned in a range of 4000–400 cm^{-1} with nitrogen purge.

3. Results and discussion

Fig. 6 presents optical images of drops of PA6 and PP on Cloisite® 30B clay disks. Recall that polymer pellets were kept on clay discs to melt at 250 °C and to assume equilibrium shape in a period of 1 h. It is seen that PP spread more on clay surface than PA6 and that PA6 exhibited much higher contact angle, ~73.5° on clay surface than PP, ~30°. This is counterintuitive as Cloisite® 30B clay is known to have more favorable interactions with polar polymer PA6, which is reflected in the production of exfoliated nanocomposites [1,2,35]. PP, on the other hand, lacks energetic interactions with Cloisite® 30B clay and produces only intercalated composites [36]. Although counterintuitive, a higher contact angle for PA6 in Fig. 6 can be attributed to chemical changes in clay and consequently a loss of polarity of clay upon heat treatment in a period of 2 h at 250 °C. As noted by other investigators [8–11], quaternary ammonium ions of clay experienced thermal decomposition during this prolonged exposure to heat and possibly chemisorbed water was removed, which resulted in alteration of surface energy of the clay particles. Note that only physi-sorbed water was removed from clay during vacuum drying at 80 °C. Table 1 shows contact angle values of PP and PA6 on heat treated Cloisite® 30B and Cloisite®NA^+ for the same duration. In the case of PP, contact angle values were determined at two temperatures −180 and 250 °C-both above the crystalline melting point of PP (165 °C). A higher value of contact angle for polar polymer PA6 on Cloisite® 30B compared to Cloisite®NA^+ can be attributed to changes in surface energy of Cloisite® 30B upon thermal decomposition of the quaternary ammonium ions. For PP, a non-polar polymer, the contact angle values at 250 °C on Cloisite® 30B is slightly lower than that on Cloisite®NA^+. This can be again explained on the basis of decomposition of the quaternary ammonium ions, which rendered clay surface much less polar.

Table 1
Contact angle values of PA6 and PP on Cloisite® 30B and Cloisite®NA+ disks

Specimen and substrate	Contact angle (°)
PA6 on Cloisite® 30B 250 °C	73.5±5.3
PA6 on Cloisite®NA+250 °C	61.2±3.3
PP on Cloisite® 30B 250 °C	30.0±1.5
PP on Cloisite®NA+250 °C	38.7±1.7
PP on Cloisite® 30B 180 °C	41.4±1.5
PP on Cloisite®NA+180 °C	33.3±1.1

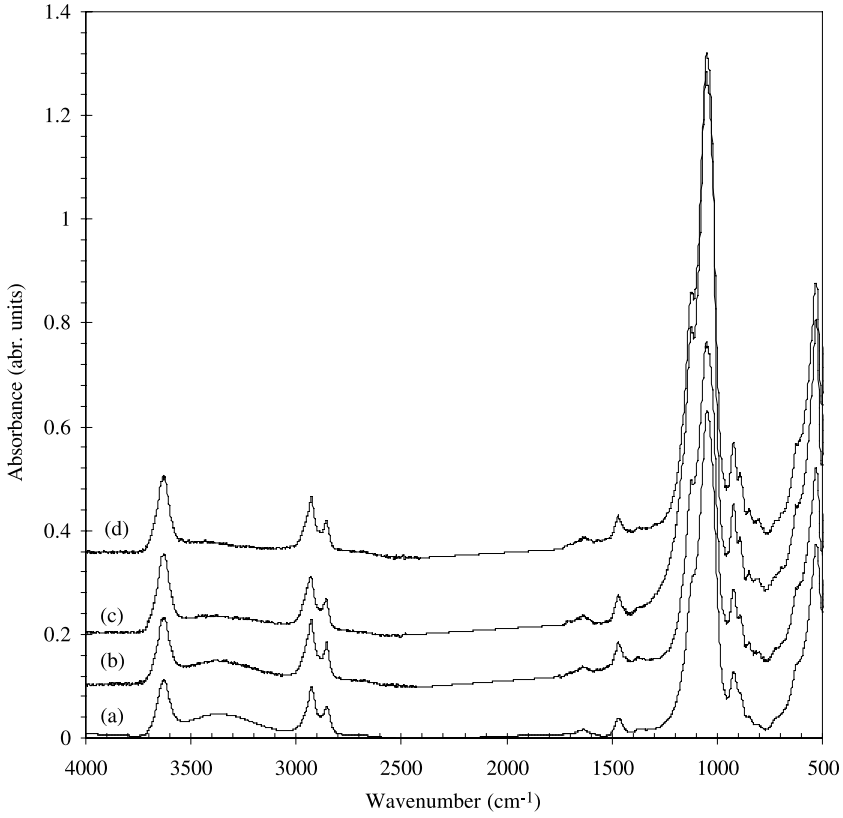

Fig. 7. FTIR scans of Cloisite® 30B surfaces. (a) clay as received, (b) treated at 220 °C for 7 min, (c) treated at 220 °C for 7 min and 250 °C for 17 min, (d) treated at 250 °C for 60 min.

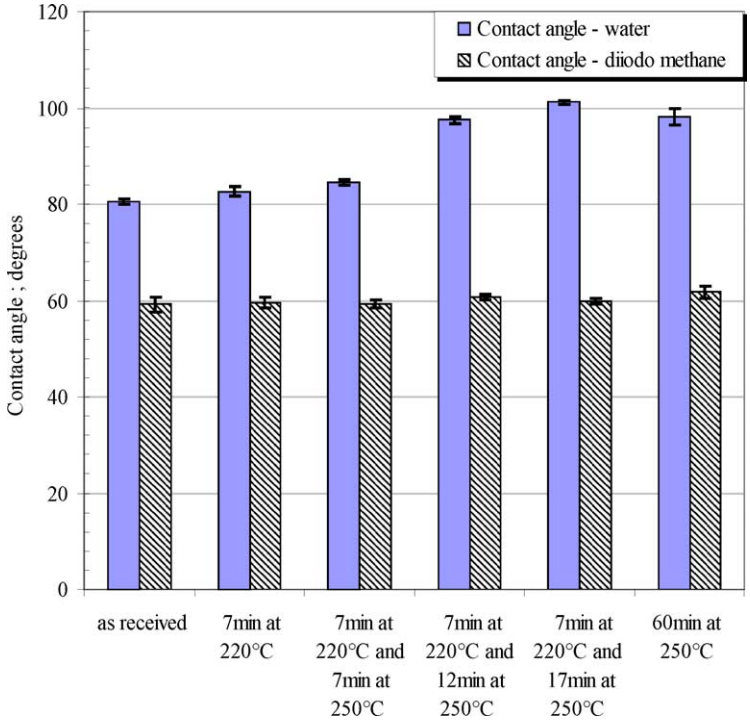

Fig. 8. Contact angle values of water and diiodomethane on heat treated Cloisite® 30B surfaces. The temperature and duration of exposure to heat is shown.

Fig. 7 shows FTIR scans of as received Cloisite® 30B (curve (a), Fig. 7) and heat treated Cloisite® 30B particles for various durations (curves (b)–(d), Fig. 7). It is seen that the peak height due to –OH stretching in region 3000–3500 cm^{-1} decreased as a result of heat treatment and almost disappeared at the longest duration (curve (d), Fig. 7). This indicates that the quaternary ammonium ions decomposed and lost polar $–CH_2CH_2OH$ groups upon heat treatment of clay. The influence of such loss of polar $–CH_2CH_2OH$ groups is further reflected in the values of contact angle of PP on Cloisite® 30B surface at two different temperatures (Table 1). The contact angle value of PP at 180 °C is higher than that at 250 °C, supporting that the organic treatment is less likely to decompose appreciably at 180 °C as noted by other investigators [8]. Note that identification of various species released by such decomposition was beyond the scope of the present work. Detailed investigations by other researchers list typical decomposition products from model alkyl ammonium ions [8–10].

The molten polymer droplet shapes in Fig. 6 and associated molten polymer contact angle values listed in Table 1 were first indication that Cloisite® 30B clay particles underwent thermal decomposition upon heat treatment. We now turn to contact angle values determined using water and diiodomethane on heat treated clay surfaces for the purposes of computation of surface free energy and polarity. Fig. 8 shows contact angle values of water and diiodomethane on heat treated clay surface. It is evident that contact angle of diiodomethane, a non-polar liquid, almost remained unchanged, while that of water, a polar liquid, increased with the increase of decomposition temperature from 220 to 250 °C and with the increase of decomposition

Table 2
Values of contact angle and energy surface components of heat treated Cloisite® 30B clay surfaces

Heat treatment protocol	Contact angle (°)		Surface energy			Polarity (p) (γ^p/γ)
	H_2O	CH_2I_2	Dispersion (γ^d) dyn/cm	Polar (γ^p) dyn/cm	Total (γ) dyn/cm	
As received	80.6	59.2	22.4	12.6	35.0	0.360
7 min, 220 °C	82.7	59.6	22.5	11.5	34.0	0.338
7 min, 220 °C; 7 min, 250 °C	84.4	59.4	22.9	10.5	33.4	0.315
7 min, 220 °C; 12 min, 250 °C	97.5	60.6	26.0	4.2	30.2	0.139
7 min, 220 °C; 17 min, 250 °C	101.1	59.9	28.6	2.3	30.9	0.075
250 °C, 60 min	98.2	61.7	25.6	4.1	29.7	0.137

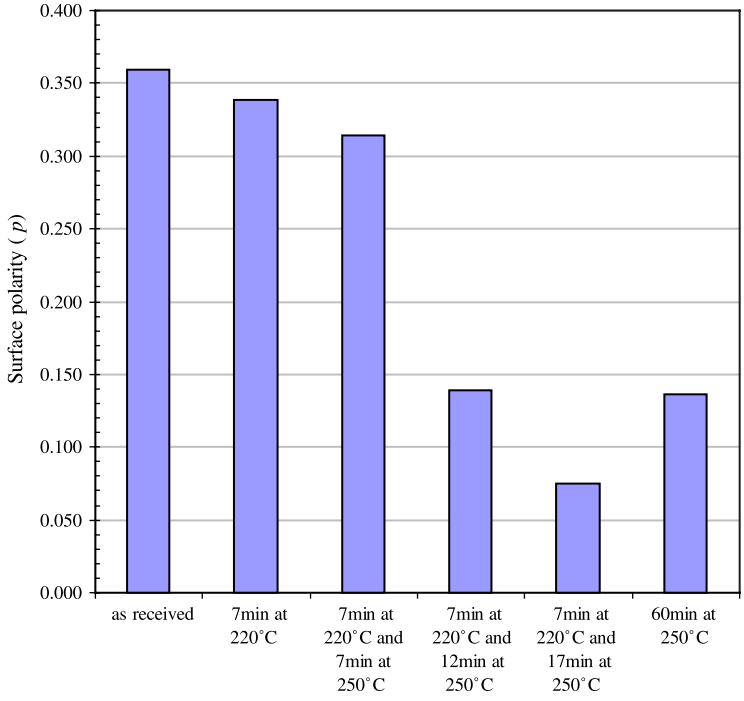

Fig. 9. Surface polarity of heat treated clay surfaces. The temperature and duration of exposure to heat are given.

time at 250 °C. The values of total surface energy (γ) and its polar (γ^p) and dispersion (γ^d) components were calculated from Wu's equation [23,24]. These are presented in Table 2. The surface polarity, which is the ratio of γ^p and γ, is plotted as function of various decomposition temperatures and duration (Fig. 9). It is seen that surface polarity of clay decreased with the duration of heat treatment—it reduced drastically after clay surface was treated for more than 7 min at 220 °C and 7 min at 250 °C. The higher values of contact angle of PA6 on Cloisite® 30B surface seen in Fig. 6 and Table 1 can now be correlated with this loss of surface polarity. It is noted in Fig. 9 that clay treated at 250 °C for 60 min has higher polarity compared to clay treated for 7 min at 220 °C followed by 17 min at 250 °C. This may be due to differences in the nature of various organic molecules generated as products of decomposition at different temperature, e.g. hydrocarbon fragments vs. carboxylic acids. This, however, was not further investigated.

The polarity and various components of surface energy of pristine PP and PA6, and PPCL compound are presented in Table 3. It is clear that the value of polarity of pristine PA6 ~0.37 is similar to that of as received Cloisite® 30B clay, ~0.36, which indicates PA6 and as received Cloisite® 30B clay are compatible in terms of surface energy as is commonly believed in literature. However, the results presented in Fig. 8 shows that these materials become incompatible while processing at elevated processing temperatures, e.g. at 250 °C for 7 min in this work. Also note that the polarity of Cloisite® 30B clay processed at 250 °C for 7 min reduced from its as received value and approached that of PP when exposed at 250 °C for 1 h. This supports why higher spreading of PP was observed on heated clay surface, as in Fig. 6.

Though polarity of the clay surface decreased substantially with thermal decomposition, the XRD analysis of these surfaces, as shown in Fig. 10, did not exhibit any such trend. The XRD scans showed that heating of clay at high temperatures resulted in a slight decrease in the gallery spacing, as revealed from the shifting of the peaks to slightly higher values of 2θ. This indicates that among XRD, FTIR, and contact angle measurements the last method is much more sensitive in capturing the effects of thermal decomposition of alkyl ammonium ions. In addition, the

Table 3
Contact angle and surface energy values of PP, PA6, and PPCL

Material	Contact angle (°)		Surface energy			Polarity (p) (γ^p/γ)
	H_2O	CH_2I_2	Dispersion (γ^d) dyn/cm	Polar (γ^p) dyn/cm	Total (γ) dyn/cm	
PP	111.0	72.9	28.3	0.0	28.3	0.000
PA6	71.8	48.7	26.1	15.6	41.7	0.373
PPCL	102.4	72.0	20.9	3.8	24.7	0.155

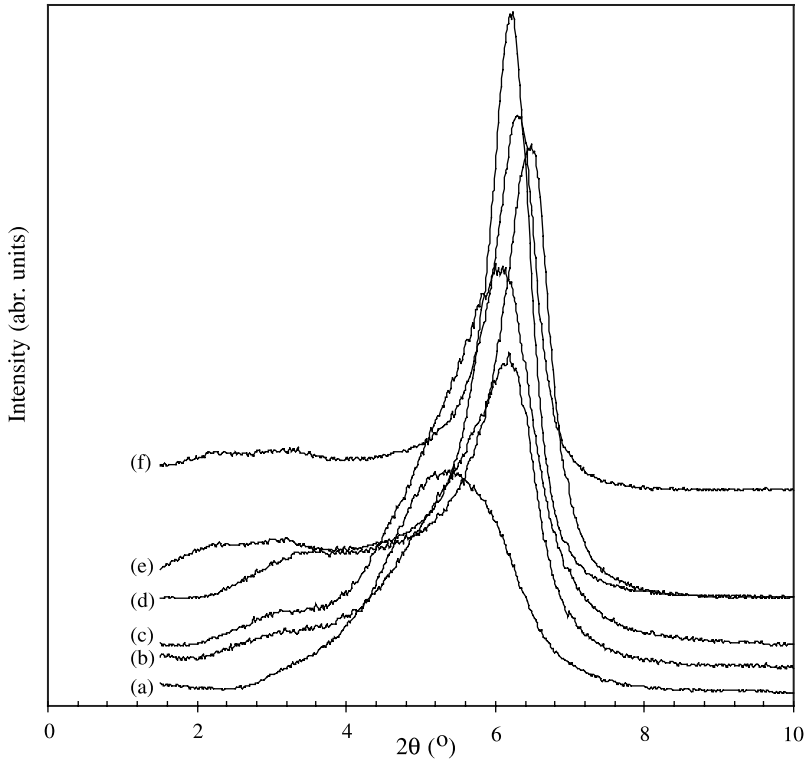

Fig. 10. XRD scans of heat treated Cloisite® 30B surfaces. (a) Clay as received, (b) treated at 220 °C for 7 min, (c) treated at 220 °C for 7 min and 250 °C for 14 min, (d) treated at 220 °C for 7 min and 250 °C for 17 min, (e) treated at 250 °C for 60 min, and (f) treated at 250 °C for 120 min.

contact angle values directly relate to compatibility between organically modified clay and the host polymer.

The values of interfacial energy between polymer pairs and clay–polymer pairs were computed as presented in Table 4. It is seen that the presence of clay in PP, i.e. in PPCL compound helped reduce the value of interfacial tension between PA6 and PP from 15.7 to 7.7 mN/m. We found similar reduction in interfacial tension using thread breakup method [30,31]. In addition, Table 4 shows that the interfacial energy value between as received Cloisite® 30B and PA6 is low, while that between Cloisite® 30B and PP is high, indicating that dispersion of Cloisite® 30B clay is much easier in PA6 than in PP. However, exposure to heat at the mixing temperature increased the value of interfacial tension between clay and PA6, while that between clay and PP decreased substantially, which now changed the scenario somewhat. In view of this, heat treated Cloisite® 30B clay may have shown more affinity to PP-phase and the trend of clay migration to PA6 phase shown in Fig. 4 may have been influenced by such change in the affinity.

Table 4
Interfacial tension values calculated using components of surface energy presented in Tables 2 and 3

Material pair	Interfacial tension (dyn/cm)
PA6/PP	15.7
PA6/PPCL	7.7
Cloisite® 30B as received/PA6	0.6
Cloisite® 30B as received/PP	13.3
Cloisite® 30B (heated for 1 h at 250 °C)/PA6	6.8
Cloisite® 30B (heated for 1 h at 250 °C)/PP	4.2

4. Conclusions

The study showed that contact angle measurement technique can be used as an effective tool to reveal if mixing temperature has any effect on clay properties. The study also showed that surface energy values are much more sensitive indicators of decomposition of alkyl ammonium ions in organically modified nanoclay than XRD scans. It was learned that changes in surface polarity of clay during nanocomposites preparation have direct influence on the affinity to various polymer components and hence on clay dispersion characteristics.

Acknowledgements

OMNOVA Industrial Fellowship to DD and the use of contact angle measurement apparatus at Omnova Solutions, Inc. are gratefully acknowledged. Authors thank National Science Foundation (NSF) for partial financial assistance in the form of CAREER grant (DMI-0134106) to SCJ.

References

[1] Usuki A, Kojima Y, Kawasumi M, Okada A, Fukushima Y, Kurauchi T, et al. J Mater Res 1993;8(5):1179–84.
[2] Usuki A, Kojima Y, Kawasumi M, Okada A, Fukushima Y, Kurauchi T, et al. J Appl Polym Sci 1993;49:1259–64.
[3] Ray SS, Okamoto M. Prog Polym Sci 2003;28:1539–641.
[4] Grim RE. Clay mineralogy 1968. p. 313–28 [see also p. 353–57].
[5] Pinnavaia TJ, Beall G. Polymer–clay nanocomposites. New York: Wiley; 2000.
[6] Cho JW, Paul DR. Polymer 2001;42:1083–94.
[7] Fornes TD, Yoon PJ, Keskkula H, Paul DR. Polymer 2001;42: 9929–40.
[8] Xei W, Gao Z, Pan W, Hunter D, Singh A, Vaia R. Chem Mater 2001; 13:2979–90.
[9] Xei W, Xei R, Pan W, Hunter D, Koene B, Tan L, et al. Chem Mater 2002;14:4837–45.
[10] Vanderhart DL, Asano A, Gilman JW. Chem Mater 2001;13: 3796–809.
[11] Davis HD, Mathias LJ, Gilman JW, Schiraldi DA, Shields JR, Trulove P, et al. J Polym Sci, Part B: Polym Phys 2002;40:2661–6.
[12] Yoon PJ, Hunter DL, Paul DR. Polymer 2003;44(18):5341–54.
[13] Fornes TD, Yoon PJ, Paul DR. Polymer 2003;44(24):7545–56.
[14] Park JH, Jana SC. Polymer 2004;45:7673–9.
[15] Gelfer MY, Song HH, Liu LL, Hsiao BS, Chu B, Rafailovich M, et al. J Polym Sci, Part B: Polym Phys 2003;41:44–54.
[16] Wang Y, Zhang Q, Fu Q. Macromol Rapid Commun 2003;24:231–5.
[17] Li X, Park HM, Lee JO, Ha CS. Polym Eng Sci 2002;42(11):2156–64.
[18] Wang S, Hu Y, Wang Z, Yong T, Chen Z, Fan W. Polym Degrad Stab 2003;80:157–61.
[19] Wang H, Zeng C, Elkovitch M, Lee J, Koelling K. Polym Eng Sci 2001;41(11):2036–46.
[20] Mehrabzadeh M, Kamal M. Can J Chem Eng 2002;80:1083–92.
[21] Tang Y, Hu Y, Zhang R, Gui Z, Wang Z, Chen Z, et al. Polymer 2004; 45:5317–26.
[22] Khatua B, Lee D, Kim H, Kim J. Macromolecules 2004;37:2454–9.
[23] Wu S, Brzozowski KJ. J Colloids Interface Sci 1971;37(4):686–90.
[24] Wu S. J Polym Sci, Part C 1971;34:19–30.
[25] Owens DK, Wendt RC. J Appl Polym Sci 1969;13:1741–7.
[26] Quayle OR. Chem Rev 1953;53:439–586.
[27] van Krevelen DW. Properties of polymers. 3rd ed. Amsterdam: Elsevier Science; 1990 [part II].
[28] Le Pluart L, Duchet J, Sautereau H, Gerard JF. J Adhes 2002;78: 645–62.
[29] www.nanoclay.com/data/30B.htm.
[30] Dharaiya D, Jana SC. J Polym Sci, Part B: Polym Phys 2005 [accepted].
[31] Dharaiya D, Jana SC. SPE ANTEC Proc 2004;62(3):2798–802.
[32] Jana SC, Sau M. Polymer 2004;45(5):1665–78.
[33] Sau M, Jana SC. AIChE J 2004;50(10):2346–58.
[34] Sau M, Jana SC. Polym Eng Sci 2004;44(3):407–22. Errata: Sau M, Jana SC. Polym Eng Sci 2004;44(7):1403.
[35] Dennis HR, Hunter DL, Chang D, Kim S, White JL, Cho JW, et al. Polymer 2001;42:9513–22.
[36] Kim KN, Kim H, Lee JW. Polym Eng Sci 2001;41(11):1963–9.